6-2021

Analysis of Possible Hybrid Meson Decay

Jasper Bergh
Union College - Schenectady, NY

Analysis of Possible Hybrid Meson $\pi_1(1600)$ Decay

By

Jasper Bergh Colin Gleason (Advisor)

* * * * * * * * *

Submitted in partial fulfillment

of the requirements for

Honors in the Department of Physics

UNION COLLEGE

June, 2021

Abstract

JASPER BERGH Analysis of Possible Hybrid Meson $\pi_1(1600)$ Decay. Department of Physics, June, 2021.

ADVISOR: Colin GleasonThis research looked at data from the GlueX experiment at the Thomas Jefferson National Accelerator Facility to search for evidence of the $\pi_1(1600) \to \eta'\pi^0$ particle, an exotic hybrid meson. We specifically looked into the $\eta \to 3\pi^0$ decay channel of the η particle for evidence of $\pi_1(1600)$. We successfully reconstructed an η from 3 π^0's, and an η' from the η, π^+, and π^-. However, we did not clearly observe $\pi_1(1600)$, but we observed nearly 6:1 ratio of signal to background in the η' mass meaning that this is a viable channel to search for hybrid mesons.

Contents

List of Figures

1 Introduction

Quantum chromodynamics (QCD) the theory of the strong iteration that describes how quarks and gluons interact. Gluons are the force carriers of the strong force, much like the photon is the force carrier in the electromagnetic force. In electromagnetism, there are two types of charge: positive and negative, whereas, in QCD, quarks have one of three color charges or one of three anti-colors: red, green, and blue, or anti-red, and-green and anti-blue. The interaction between one gluons of one color and its corresponding anti color is somewhat similar to positive and negative change in electromagnetism. Quarks also have an electric charge, up quarks for example have a charge of $+2/3$, while down quarks have a charge of $-1/3$. Gluons, on the other hand, have no electric charge but do carry a color charge that allows for gluon–gluon interactions, this is a large difference from electromagnetism, where photons have no change and do not interact directly with each other. Two important properties of QCD are color confinement and asymptotic freedom. Color confinement simply states that no color–charged particle (gluons and quarks) can exist in isolation. Therefore, quarks and gluons cannot be observed directly, only when they are grouped to form hadrons. Asymptotic freedom describes the quarks at different energy, or length, scales. At high energies, perturbative calculations can be used to describe the interaction between quarks. At low energies, quarks become confined inside of hadrons and perturbative calculations can not be used to describe the interaction.

Hadrons are particles built from quarks that are held together by gluons. Baryons are hadrons that are three quarks of differing color charge, for example, the Proton with flavor (up, up, down) and Neutron (up, down, down) are both baryons. Mesons are hadrons that have 2 quarks in a quark anti-quark ($q\bar{q}$) pair. A common example of a meson in the π^+ particle, which is an up quark and an anti–down quark. Mesons can be categorized by their total angular momentum J, their parity symmetry, P, and their charge symmetry C, commonly written as J^{PC}. In the typical $q\bar{q}$ model of a meson, only certain configurations of J^{PC} can exist, $J^{PC} = 0^{-+}, 0^{++}, 1^{++}, ...$, others configuration are not allowed by the properties of the J^{PC} quantum numbers when there is only a standard quark- antiquark pair.

Configurations of J^{PC} outside of the standard $q\bar{q}$ picture are called "exotic mesons". These configurations are $J^{PC} = 0^{--}$, any odd integer^{-+}, and any even integer^{+-} [7]. Of these particles, hybrid mesons appear when there is the standard $q\bar{q}$ pair along with an excited gluonic field that has non–negligible properties. This means that in addition too the quarks in the meson there is an excited gluonic field that contributes to the J^PC quantum number in some way.

There is a broad spectrum of hybrid mesons predicted by Lattice QCD [5], a way of solving QCD. Figure 1 shows the mass of the predicted meson as a function of its J^{PC}. The left and middle columns represent mesons that have quantum numbers that can be built from $q\bar{q}$, and the right column represents mesons that

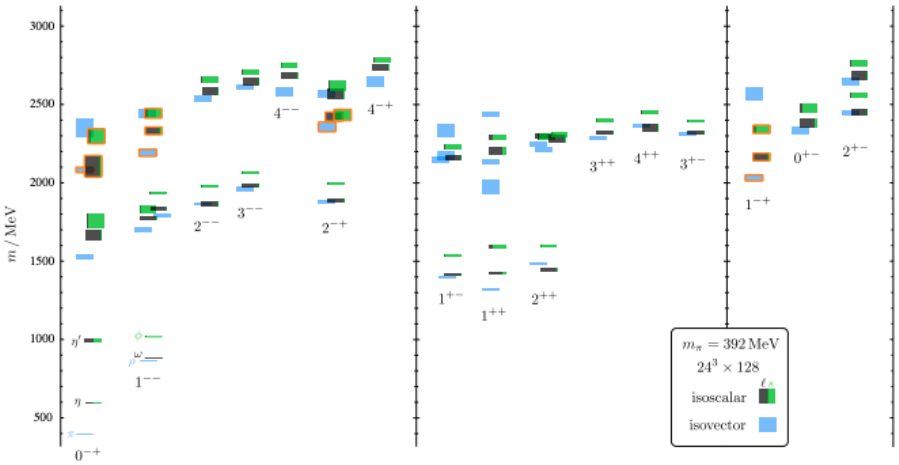

Figure 1: The spectrum of mesons predicted by lattice QCD [5].

have exotic quantum numbers. The states highlighted in orange correspond to particles that have gluonic excitations. The three states highlighted in the right column correspond to hybrid mesons with exotic quantum numbers. The lowest mass state with quantum numbers 1^{-+} would correspond to the $\pi_1(1600)$

The COMPASS (Common Muon and Proton Apparatus for Structure and Spectroscopy) experiment at CERN[2] has shown evidence of a light exotic hybrid meson with quantum numbers $J^{PC} = 1^{-+}$, in the decay system $\eta'\pi^-$. This particle is named $\pi_1(1600)$. This particle appears in the right column of Figure 1 as the lowest-lying hybrid state.

There have been other efforts to measure the $\pi_1(1600)$, mainly using the $\eta'\pi$ system. Currently, the GlueX Experiment at Jefferson Lab[1] is searching for the $\pi_1(1600) \rightarrow \eta'\pi$. Efforts have primarly been focused on reconstructing η''s that decay to $\eta\pi^+\pi^-$ and $\eta \rightarrow \gamma\gamma$. In this work, we looked at the $\eta \rightarrow \pi^0\pi^0\pi^0$ decay. The larger number of final–state particles typically leads to fewer events that can be reconstructed. Additionally, the $\eta \rightarrow \pi^0\pi^0\pi^0$ decay has a lower branching ratio. According to Particle Data Group (PDG), η decays into two photons ($\gamma\gamma$) approximately $(39.41 \pm 0.020)\%$ of the time, whereas it decays into three pions ($\pi^0\pi^0\pi^0$) approximately $(32.68 \pm 0.023)\%$ of the time [9].

2 GlueX Experiment setup

2.1 Jefferson Lab

The Gluonic Excitation (GlueX) experiment [1], located within the United States Department of Energy's Thomas Jefferson National Accelerator Facility (JLab), is an experiment in the search for exotic hybrid mesons. Figure 2 shows a schematic of the experimental setup at Jefferson Lab. Jefferson Lab is home

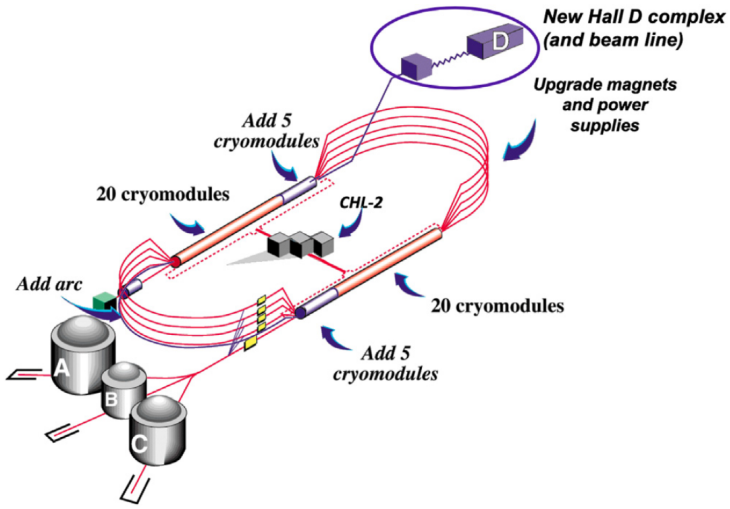

Figure 2: Continuous Electron Beam Accelerator Facility (CEBAF) at JLab facility, GlueX is located in Hall D. Taken from [1].

to an electron accelerator and four experimental halls. Electrons can be accelerated up to 12 GeV and can be simultaneously delivered to the experimental halls.

2.2 GlueX

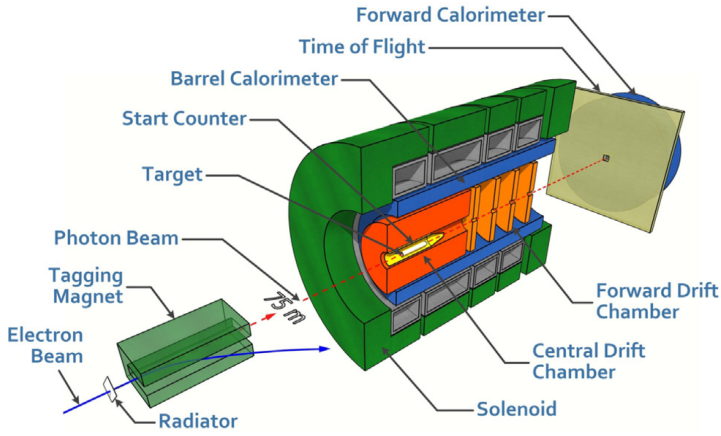

Figure 3: The Setup of the GlueX Experiment. Taken from [1].

The basic setup for the GlueX Experiment is a 12–GeV linearly-polarized photon beam, incident on a proton target, Figure 3 shows a setup of the experiment [1]. The incident photon beam is produced from an accelerated electron beam, which is fed into a 50 μm thick diamond crystal radiator, producing linearly-polarized photons. The electrons are then curved away using a powerful magnetic field to be detected. The detected electron energy is then used to determine the energy of the photon beam. The photon beam

continues down the beamline where it can interact with the proton target. Scattered particles are then measured by a series of detectors around the target.

A large solenoidal magnet surrounds the detector and bends charged particles towards or away from the beamline. Drift chambers track the movement of charged particles inside the detector, which deposit energy in the electromagnetic calorimeters. Two electromagnetic calorimeters are used to identify particles, one surrounding the proton target, and one downstream of the beam. The entire detector is nearly hermetically sealed off to lower detection of background particle interference. This allows for the reconstruction of energy and momentum. The time of flight of a particle is used to measure the timing of charged particles.

3 Results

3.1 Reaction Overview

The goal of this research project was to look for the hybrid meson candidate $\pi_1(1600) \rightarrow \eta'\pi^0$ in the reaction $\gamma p \rightarrow Xp \rightarrow \eta'\pi^0 p$. Before we can search for the $\pi_1(1600)$, we need to show that we can reconstruct the η', the π^0, and their decay products. Figure 4 shows a schematic of the reaction we analyzed. An incoming photon will interact with a proton (p) target. For this analysis, we searched for the $\pi_1(1600)$, labeled as X, decaying into an η' and π^0. The η' then decays to $\eta\pi^+\pi^-$; the η will then decay to $3\pi^0$'s; finally all the π^0's decay to two γs. This means there will be 8 γs and 3 charged tracks (π^+, π^-, and a p) for a total of 11 final–state particles. The main challenge of this analysis was in reconstructing the η and η' as they decay to many particles, so there is less data to work with.

Current analysis efforts within the GlueX Collaboration have focused on decays of the η to 2γ's. This reaction is much simpler in that it only has four final–state photons. The decay of the $\eta \rightarrow 3\pi^0$ is the second largest neutral decay mode of the η and will have much more background due to the larger number of final–state particles, this is the specific decay we are looking at. Therefore, a primary goal of this analysis was to see if η' can be reconstructed and estimate the signal to background ratio. Ultimately, GlueX will need to observe the decay of the $\pi_1(1600)$ across multiple decay modes in order to prove its existence.

3.2 Initial Event Selection

All of the data analysis was done using the data analysis framework ROOT by CERN [4]. Data analysis was done by building back up the particles in reverse order, first doing some initial event selection and then cutting and selecting data to find the π^0's then the η and η'. The data file consists of approximately 4.3 million data points, each with properties for each of the 11 particles.

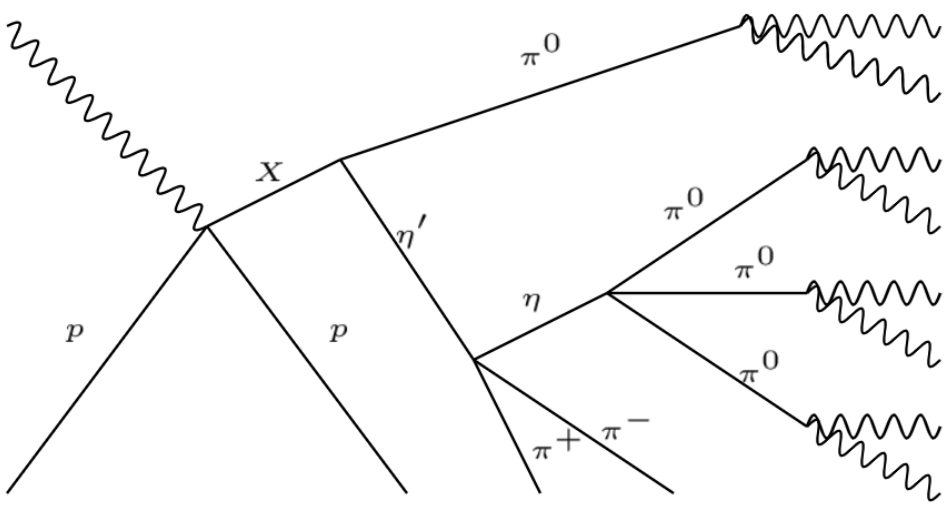

Figure 4: Diagram of the entire decay chain. The incoming high energy photon and proton are on the left. The particle we are trying to look at is labeled X.

The data set comes from GlueX's 2017 run period, which is approximately 1 petabyte of data, or 15 billion events. Before any of the plots were made, events that did not have the particles of interest (8 photons, 3 charged particles) were removed from the analysis, leaving approximately 4.3 million events. Then, a series of cuts was performed to reduce contributions from other sources of background. One such cut is a particle identification (PID) cut that is used to remove particles that originate from the wrong event. Figure 5 shows one of the timing distribution of one of the photons in the reaction. The time t is the event start time at the vertex and the time the particle hits the forward calorimeter (FCAL) detector. The event distribution over Δt is expected to be centered at zero when the assumed mass is the true mass of the particle that had produced the track. Photons whose Δt is greater than 2.5 ns were cut from the analysis. Similar cuts were made on the proton and pions.

Additional cuts were made that include removing events that originate outside the GlueX target, photons whose shower quality score was less than 0.5, and an unused energy cut of 0.1 GeV. The shower quality score is a machine learning algorithm that uses properties of the shower in the FCAL to reject events that do not come from photons [3]. It assigns a number between 0 (bad event) and 1 (good event). The unused energy cut selects events which do not have any "missing" energy, ensuring that the events only include 8 photons, a π^+, π^-, and a proton.

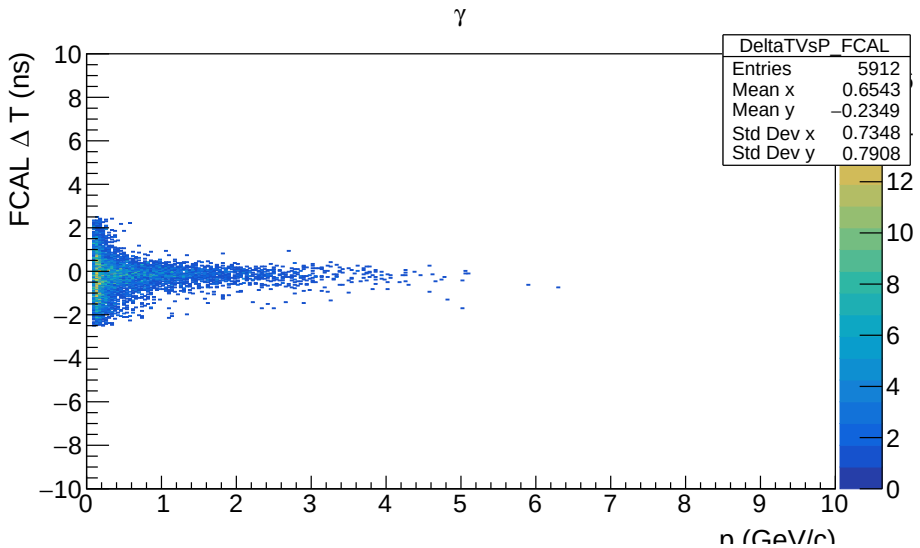

Figure 5: Histogram of Δt vs. p for one of the photons

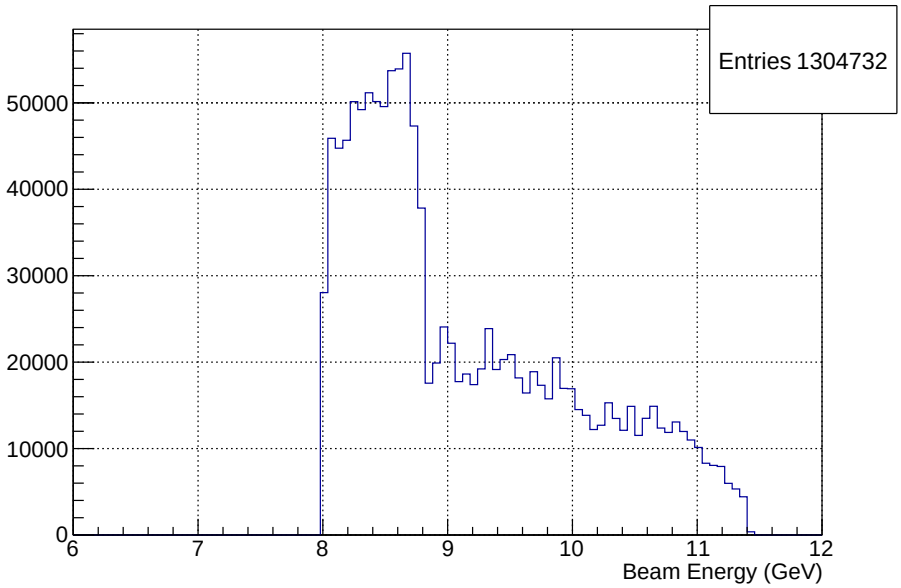

Figure 6: Histogram of the GlueX photon beam energy.

3.3 Vertex Selection

The GlueX detector is capable of detecting beam photons with energies of 4–12 GeV. Beam photons with an energy of less than 8 GeV were initially vetoed from the analysis as they typically lead to an increase in background. Figure 6 shows the photon beam energy spectrum The enhancement from 8–9 GeV corresponds to the "coherent peak" region. One unique feature of GlueX is that the photon beam is linearly polarized. This polarization can be used to study how mesons can be produced. Photons in the coherent peak region have the largest degree of linear polarization. Since the polarization is not currently used in

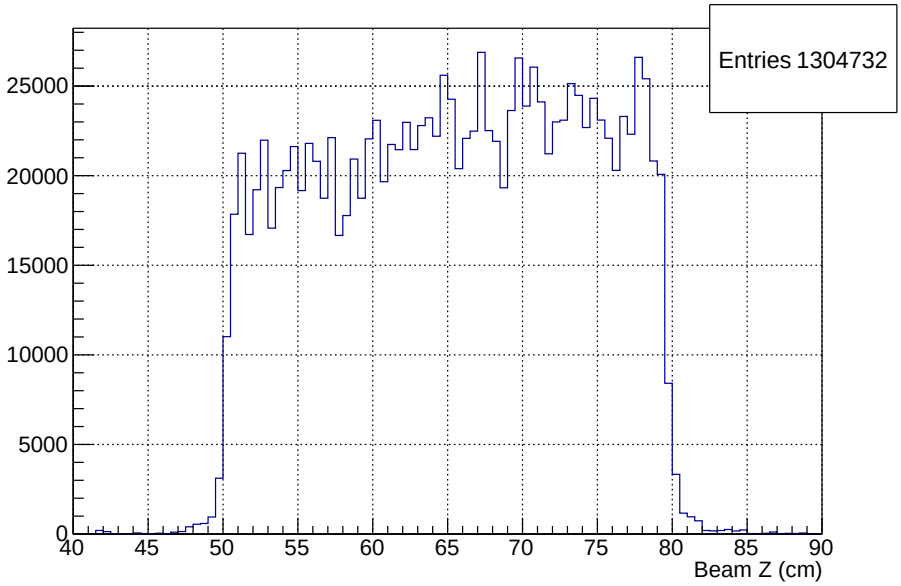

Figure 7: Histogram of the event vertex.

this analysis, all beam photons with energy of 8-9 GeV were kept.

Figure 7 shows the position of the event vertex. GlueX uses a 30–cm long LH_2 (liquid hydrogen) target for its proton target, located at position 30-80cm on the Beam-z. Events were selected if they occur between 52 cm and 78 cm. This cut was chosen to remove events that originate close to the ends of the proton target.

3.4 Kinematic Fit

Before any further analysis was done I looked at the performance of the kinematic fitter. The kinematic fitter is used to improve the resolution of the GlueX detector by imposing conservation of energy and momentum constraints between the initial and final–state particles. Each event is assigned a probability that calculated from χ^2/NDF of the kinematic fit. Events with a high probability of being "good" events occur when the $\chi^2/NDF = 1$. Events with a low probability get assigned a higher χ^2/NDF. Figure 8 shows χ^2/NDF for the events in the reaction. Events with a $\chi^2/NDF > 8$ were removed from analysis as studies from other reactions have shown this to be a good starting point. The cutoff of 8 was chosen because it still leaves many particles, while cutting out the very unlikely ones. Ideally, one would have to optimize this cut by looking at signal to background ratios.

3.5 t Channel Selection

Another quantity that can be used to enhance the reaction of interest is the t-channel Mandelstam variable. The Mandelstam variables are quantities that contain information about the energy and momentum

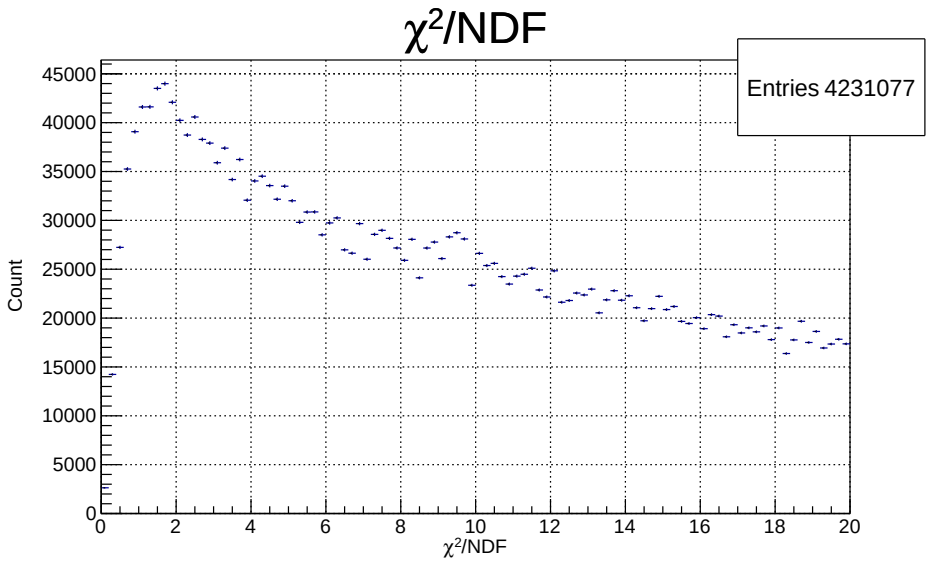

Figure 8: Histogram of χ^2 per degrees of freedom, all events greater than 8 are skipped

of reaction of interest. If the reaction we are interested in looks like $p_1 p_2 \rightarrow p_3 p_4$, where p_{1-4} are the 4-momentum of the particles of the interaction. The t channel variable can be calculated as,

$$t = (p_4 - p_2)^2 = (p_1 - p_3)^2 \tag{1}$$

In the this particular reaction, $p_1 = \gamma$, p_2 is the target proton, $p_3 = \pi_1(1600)$, and p_4 is the final–state proton. This process occurs when the initial γ emits a particle to become p_3. The emitted particle would then be absorbed by the target proton.

Figure 9 shows the $|t|$ distribution. A smaller value of t corresponds to a larger momentum transfer to the outgoing unknown particle. Very small values of t are not detected by GlueX as the proton does not have enough momentum to make it through the detector. Typically, large values of t represent the production of an excited baryon which is an undesired result for this reaction. Data–points were then skipped where $t > 1$, slightly reducing the amount of data but mainly filtering out background events.

3.6 π^0 Identification

In this data set, each pair of photons is the result of a π^0 decay. Figure 10 shows the mass of each of the pi^0's. It is known that the mass of a π^0 particle is approximately 143 MeV, so any π^0 with mass outside the range $100 - 170$ MeV is also cut out [9]. Figure 11 shows the mass of the π^0's after the mass cut.

In this data set it is known that the first two photons combine to from a pion that results from the decay of the unknown particle ($\pi_1(1600)$), whereas the other 6 photons are combined into pions that are a result

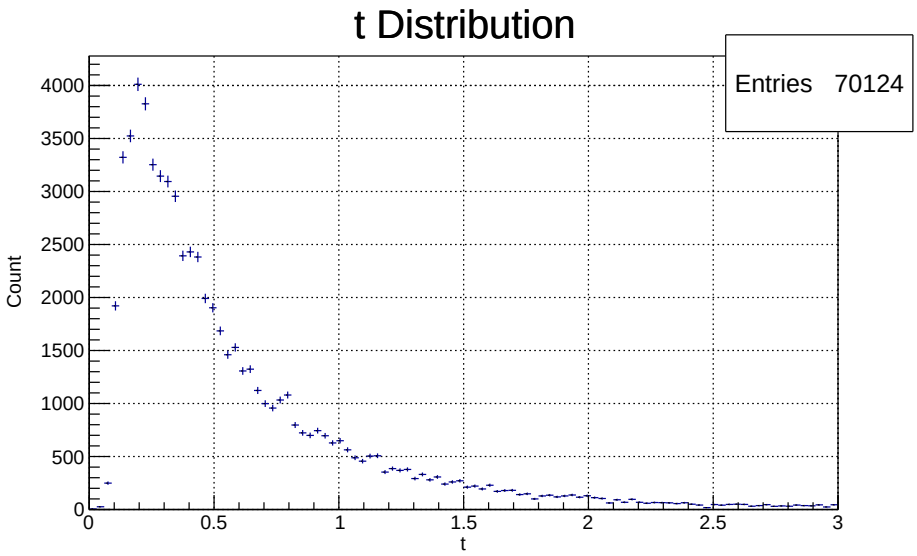

Figure 9: Histogram of the t channel Mandlestam variable of the scattering

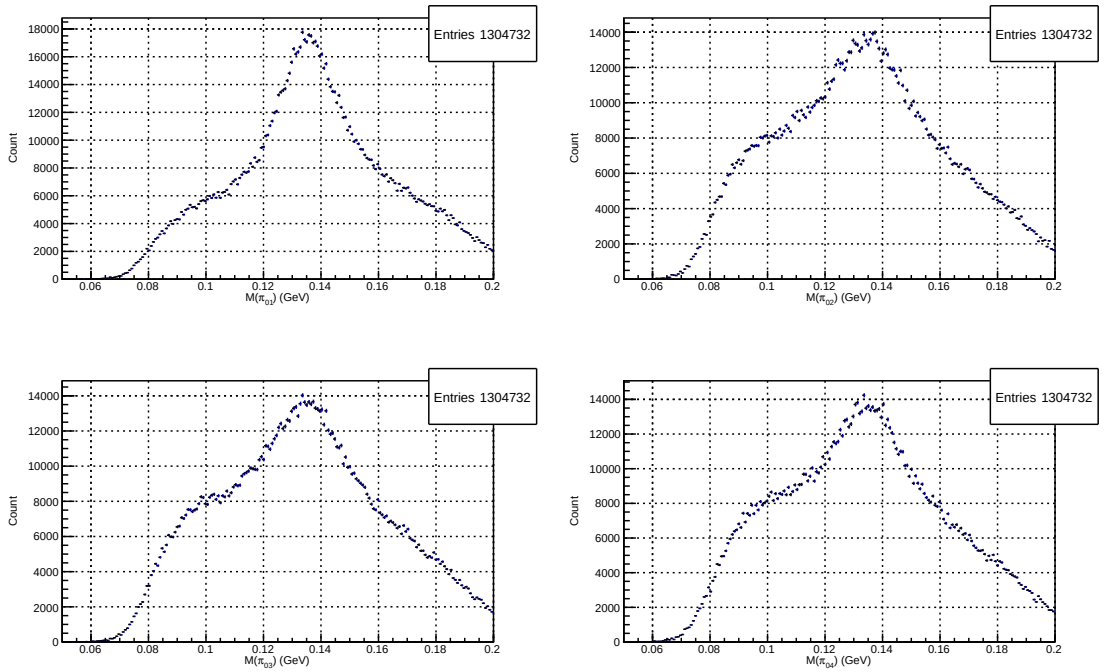

Figure 10: Mass of all 4 π^0's with no Cuts.

of the η particle decay. In this data, π_1^0 gets assigned to photons 1 and 2, π_2^0 to photons 3 and 4, π_3^0 photons 5 and 6, and π_4^0 photons 7 and 8. Therefore, we want to veto any "false" π^0's. This means we do not want any two photons that didn't originate from the same π^0 to add together and have a mass comparable to that of π^0, in the range $100 - 170$ MeV. For example if γ_1 and γ_3 added together have a mass of 140 MeV that data point would be cut because γ_1 and γ_3 should not combine to form a π^0. Figure 12 shows the mass of γ_1 and γ_3. An enhancement can be seen at approximately 140 MeV that corresponds to a π^0. Since γ_1 and

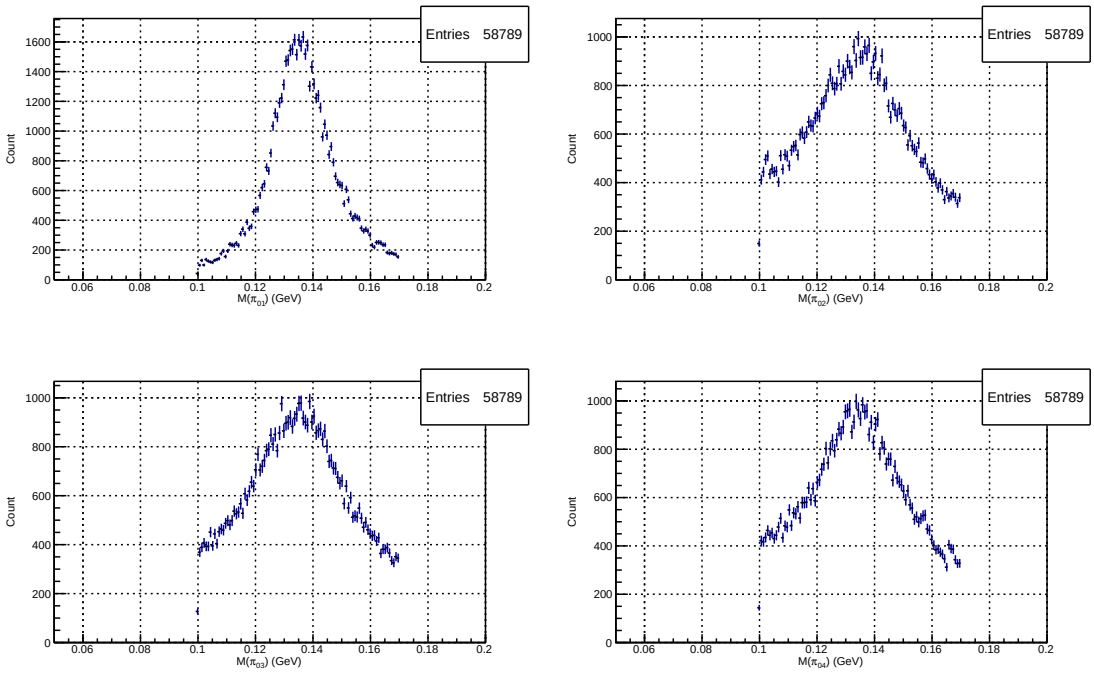

Figure 11: Mass of all 4 π^0's. Cuts were made at 0.1 and 0.17 GeV, and any false π^0 when made with γ_1 were also cut

γ_2 also combine to form a π^0, the events where γ_1 and γ_3 also form a π^0 need to be removed from analysis. Initially this vetoing was done will all combinations of photons that were part of the same π^0. However, this drastically reduced the amount of data points. Instead, only false combinations with γ_1 were vetoed from the data. This vetoing was sufficient at removing these false events, as seen by the mass of the resulting η particle.

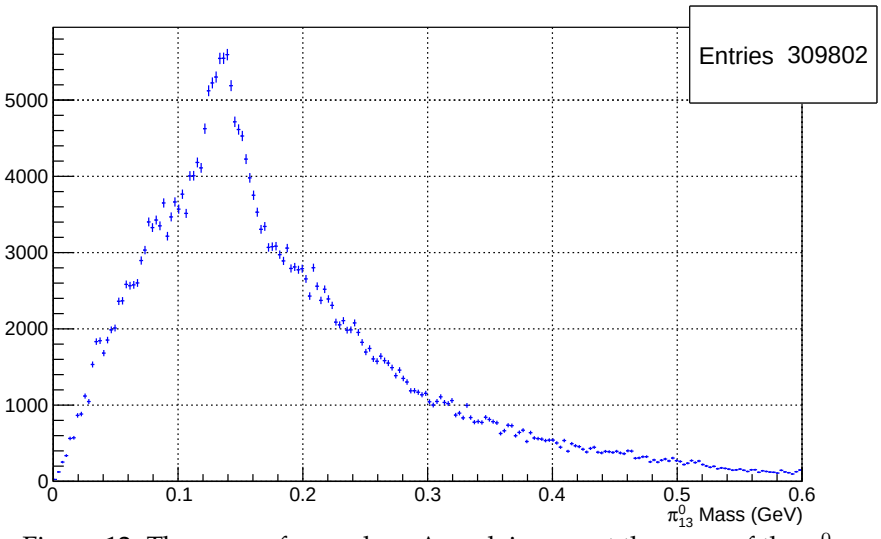

Figure 12: The mass of γ_1 and γ_3. A peak is seen at the mass of the π^0.

3.7 η Selection

After the π^0's were selected, the next step was to see if an η could be reconstructed. The η particle in this reaction decays into $\pi_2^0, \pi_3^0, \pi_4^0$. The η was reconstructed from the data by adding the four–vectors of $\pi_2^0,\ \pi_3^0$, and π_4^0. According to Particle Data Group(PDG) [9], η has a mass(M) of 547.862 ± 0.017MeV, and a width(Γ) of 1.31 ± 0.05 keV. Figure 13 shows the mass of the η prior to any π^0 selection. There is a maximum at approximately where the η is expected to be. However, it is impossible to tell how much of this is signal and how much is background, prior to selecting the pi^0's.

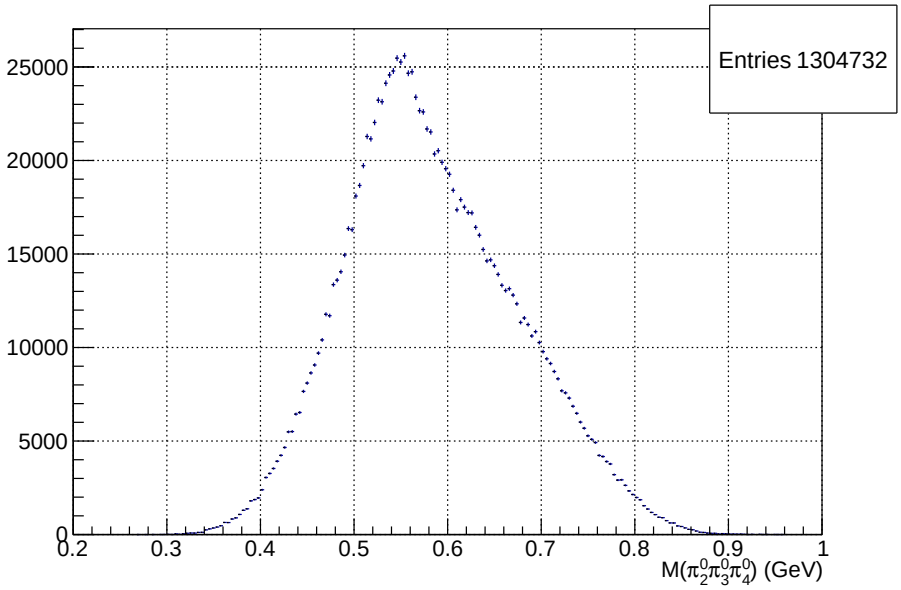

Figure 13: Mass of $\pi_2^0\pi_3^0\pi_4^0$ prior to selecting the π^0s.

Figure 14 shows the mass of the combination of the η after selecting the correct π^0's. A clear peak at approximately 555 MeV, which corresponds to the η, now sits atop a small background. This distribution is then fit with a Relativistic Breit–Wigner distribution plus a quadratic background function ($BW(x) + l_2x^2 + l_1x + l_0$). The mass of eta was found to be 549 ± 1 MeV, within the accepted value for mass. From this data the ratio of events to background at the park is about 7.14 to one; that is, for every 1 background event seen at the η mass, there is approximately 7.14 total events.

3.8 η' Selection

The η' particle decays into a combination of η, π^+ and π^- which can then be reconstructed from their four–vectors. Figure 15 shows the η' mass prior to the selection of the η and π^0s. A possible enhancement at the mass of the η' can be seen. However, this is hardly of any significance as the background it sits atop

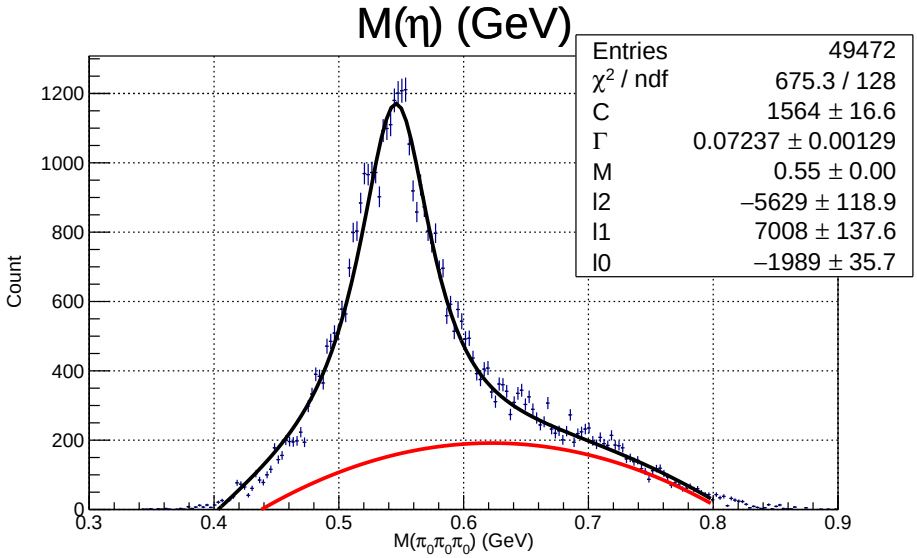

Figure 14: Mass of $\eta = \pi_2^0\pi_3^0\pi_4^0$. The distribution is fit with a Relativistic Breit–Wigner for the signal and a quadratic background function(shown in red). At the peak the ratio of events to background is 6.13 to one.

is very large in comparison to the total number of events.

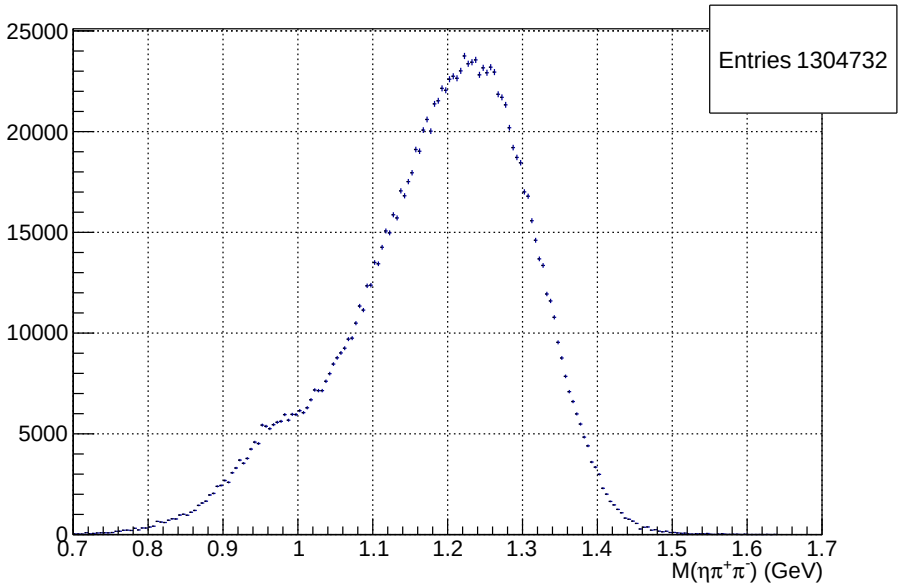

Figure 15: Mass of $\eta\pi^+\pi^-$ prior to selecting the η and π^0s.

Figure 16 shows a two dimension histogram of the η' mass as a function of the η mass after the η and π^0s are selected. A clear enhance is now seen around $M(\eta') \approx 0.95$ GeV and $M(\eta) \approx 0.55$ GeV. This corresponds to events where the η is one of the decay products of the η'. Figure 16 also shows that the η' can only be seen in the range $0.5\text{GeV} < M(\eta) < 0.6\text{GeV}$. The upward slope of the peak demonstrates that a larger η Mass corresponds with a larger η' mass, as the η is one of the η' decay products. Events in this $M(\eta)$ window far

away from the η' mass correspond to events where we have an η that does not come from the decay of the η'. These events would be considered background events. For example, they could come from the reaction $\gamma p \to \eta\pi^0\pi^+\pi^- p$ which can have many different intermediate particles.

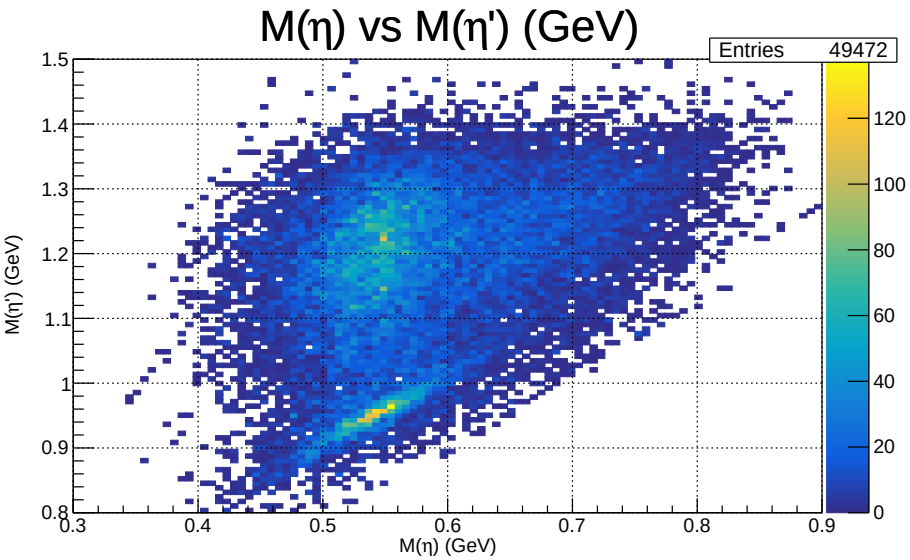

Figure 16: Mass of η vs mass of η', both in GeV. The peak at the bottom of the histogram corresponds with the η' particle.

One such possibility of particles other than η' in the reaction is the widely studied ω meson. The ω has a mass of 782.65 ± 0.12GeV and most commonly decays into $\pi^+\pi^-\pi^0$[9]. All of these resulting particles are present in our data set. If this particle were to be present in the data then there would be a spike in the plot of $\pi^+\pi^-\pi^0$ mass, which can be cut out if necessary. Figure 17 shows the $\pi^+\pi^-\pi^0$ mass. There is a clear peak where the ω particle is. Removing the ω, by cutting out all data points from 0.7-0.8 GeV from the η' mostly reduces the the amount of background and eliminates this process from the data.

Another possible cut to be made in in filtering out the Δ baryon $m \approx 1232$ MeV, which most commonly decay into a proton and a pion. In this decay chain it would be possible for the incoming proton and photon to form a Δ^+ instead of a hybrid meson. This process would occur in the s channel of the Mandelstam variables. Figure 18 show the combination of $p\pi^+$ and $p\pi^-$, both which result from a Δ decay. There is a slightly noticeable peak at the mass of the particle, however the peak is so small that no cuts on the data were deemed necessary. There may be other particles interfering with this decay chain like the Δ^+ and ω, however the resulting reduction we got from only eliminating ω appears to be sufficient.

Once the cuts on the η mass had been made and ω cut out, the resulting η' distribution can be made. Figure 19 shows the mass of the η' after this event selection. The distribution is fit with a Relativistic Breit–Wigner with only a liner background fit. Only a linear background fit was made because there is less data to work with and the η' mass is on the side of the background distribution, which is mostly linear.

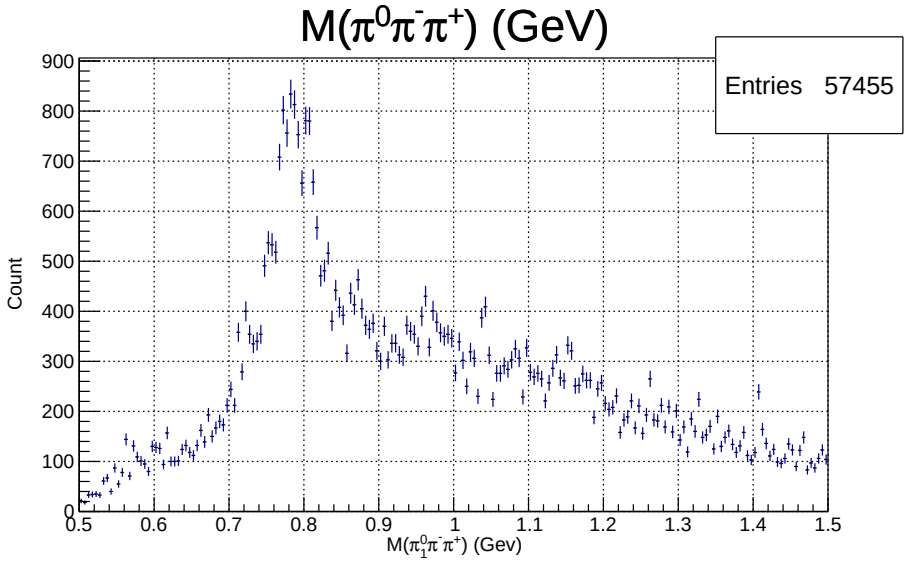

Figure 17: Mass of $\pi^+\pi^-\pi^0$, the peak at 0.7-0.8 GeV corresponds to the ω particle.

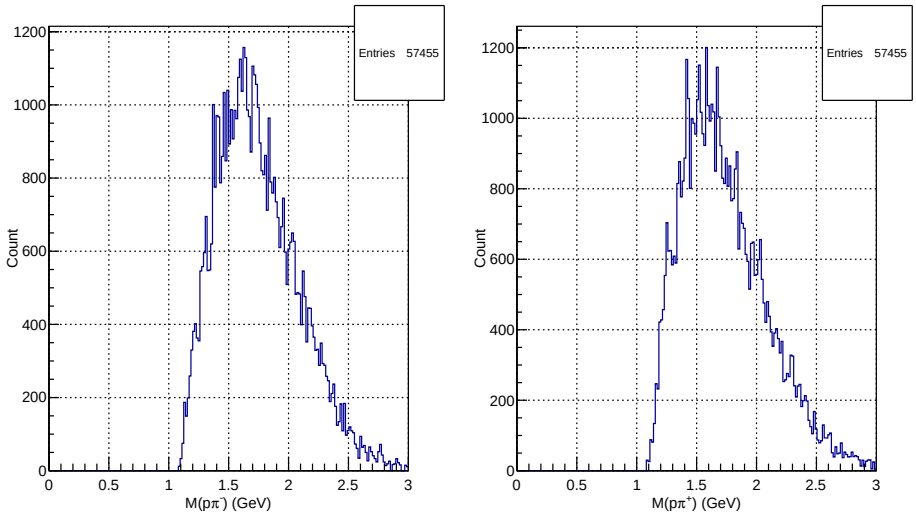

Figure 18: Mass of $p\pi^+$ and $p\pi^-$, the small peaks at approximately 1.25 GeV corresponds to the Δ^+ particle.

Surprisingly, there is a very clear peak in the mass with a ratio of signal to background of about 6. The measured mass comes out be me 958 ± 1 MeV, compared to the PDG value of 957.78 ± 0.06 MeV.

3.9 $\pi_1(1600)$ Search

Since there is a clear signal for the η', the $\pi_1(1600)$ can be reconstructed from the last π^0 and η'. The mass of η' was selected by removing events where $M(\eta')$ was above 1.04 GeV. Figure 20 shows the mass of the $\eta'\pi^0$. One of the goals of this study was to search for decays of the hybrid meson $\pi_1(1600)$ decaying to $\eta'\pi^0$. The first thing to looked at is enhancements in the $\eta'\pi 0$ mass around 1.6 GeV. Figure 20 appears to

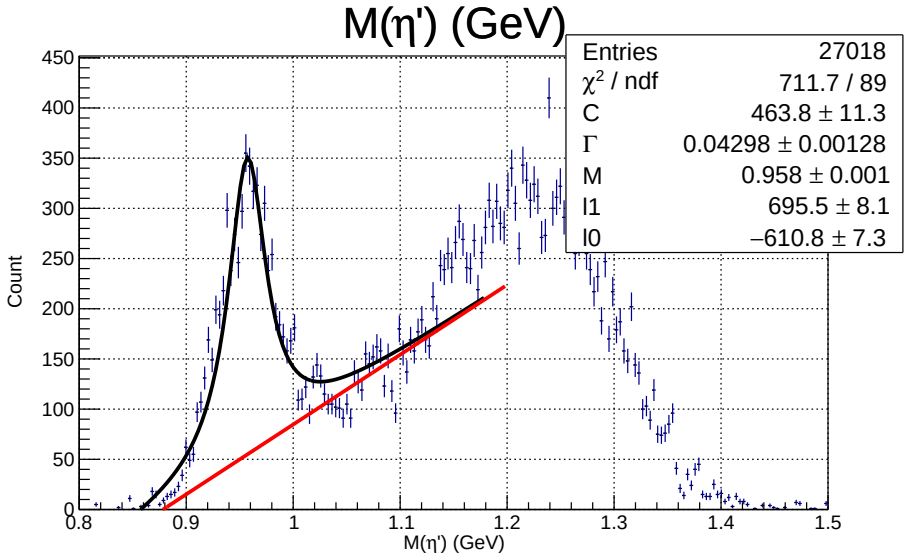

Figure 19: Mass of η' Fit with a Breit-Wigner Distribution plus a linear background fit(shown in red).

have two peaks, one at approximately 1.6Gev and one at approximately 2.2 GeV. While it is encouraging that we see enhancements in this mass region, more studies need to be done to confirm the nature of the enhancement. Additionally, the statistics are limited and changing the data selection process can change what this distribution looks like. The nature of this enhancement at approximately 2.2 GeV is unknown, although the PDG suggest there may be an a_4 particle in this mass region.

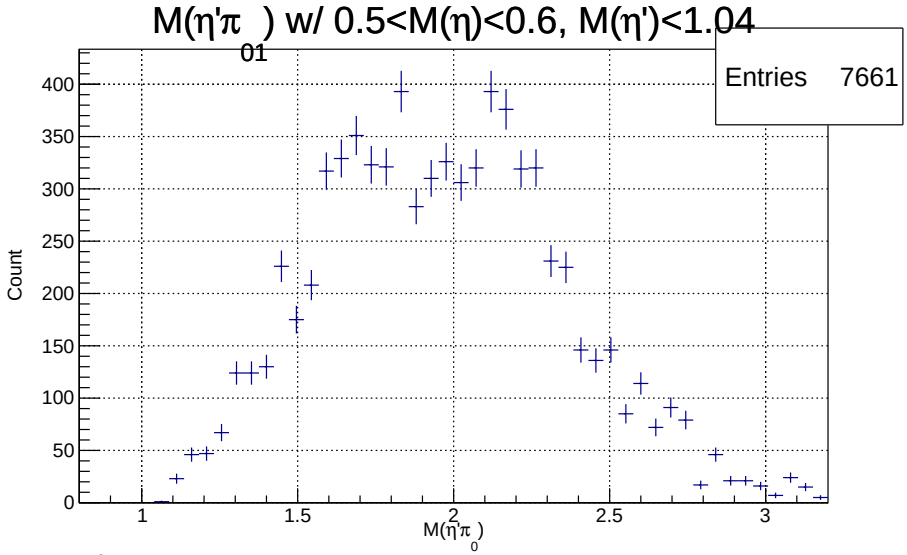

Figure 20: Mass of $\eta'\pi^0$ with $M(\eta') < 1.04$, the particle that is predicted to be $\pi_1(1600)$, which can be seen as the peak at 1600 GeV. The second peak to the right is most likely background. However there is not enough data to confirm that the histogram shows $\pi_1(1600)$

A possible cause of these enhancements could be due to not subtracting the background underneath the η' mass distribution. Figure 21 shows the $\eta'\pi^0$ mass when the η' is not selected. This would correspond

to background underneath the real η'. Here, we see an enhancement in the background at approximately 1.7 GeV, which is in the same region as we saw in the η' signal. This means that the enhancement we see around 1.6 GeV in the $\eta'\pi^0$ mass could be generated by the background. Further studies would need to be done to determine the nature of this state.

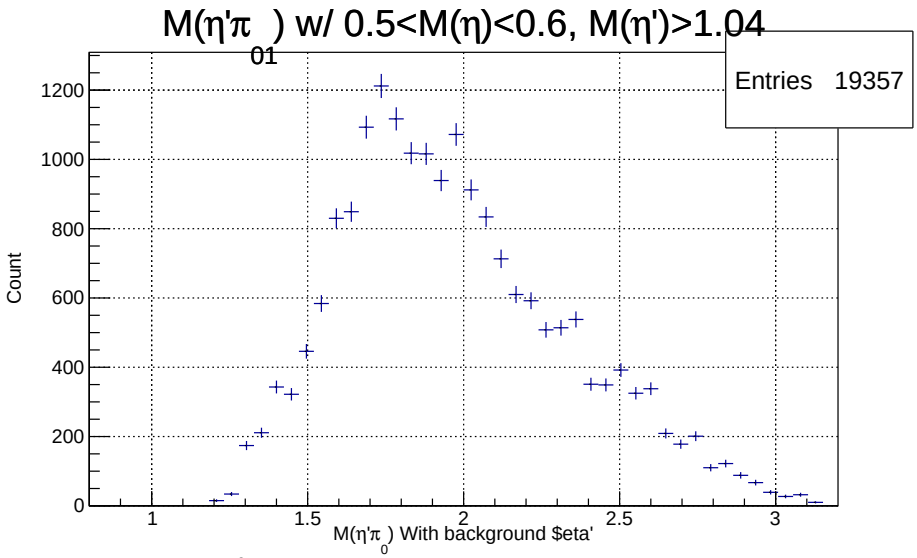

Figure 21: Mass of $\eta'\pi^0$, with $M(\eta') > 1.04$ This is all of the background from the η'.

One last step of analysis is to convert the reference frame to a Gottfried-Jackson Frame (GJ) to perform angular analysis. The GJ reference frame is defined in the center of mass frame of the $\eta'\pi^0$ system. The z-axis is the momentum of the incoming photon in the center of mass of the reaction. The y–axis is defined as the cross product between the z–axis and the $\eta'\pi^0$ momentum in the center of mass frame. The x–axis is then perpendicular to y and z. From that, the angle (θ) is the angle between the η' momentum in the GJ frame and the z-axis. This angle can be used to determine what the angler momentum J quantum number is. Theoretically, differing J quantum numbers should produce spherical harmonics.

Figure 22 shows the $\cos\theta$ distribution of the data. This histogram show the bias to the forward direction, which make sense as the detector is more likely to detect particle in the positive z–direction. Figure 23 shows $\cos\theta$ as a function of the $\eta'\pi 0$ mass. There is a broad enhancement from approximately $1.5 - 2.0$ GeV in the $\eta'\pi^0$ mass. The $\pi_1(1600)$ has $J = 1$, which would show up as enhancements at $cos\theta = \pm 1$ or an enhancement at $cos\theta = 0$. However, Figure 23 shows a roughly flat distribution in this region, Which corresponds to the $J = 0$ spherical harmonic.

One issue present in the data in Figure 23 is that we have not accounted for the acceptance of the detector. Since the detector is not perfect and does not cover all of the allowed phase space, some events can not be detected. This may explain why there are more events at $\cos\theta \approx 1$ than there are at $\cos\theta \approx -1$. The detector

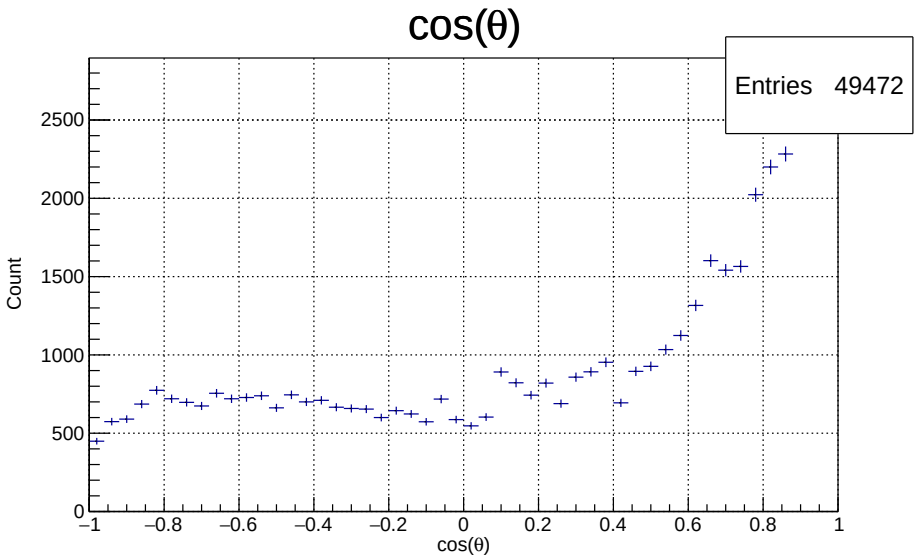

Figure 22: $\cos(\theta)$ of the η' particle in the Gottfried-Jackson Frame, The bias towards $\cos(\theta) = 0$ is caused by the detector being more much more likely to detect particle in the forward direction.

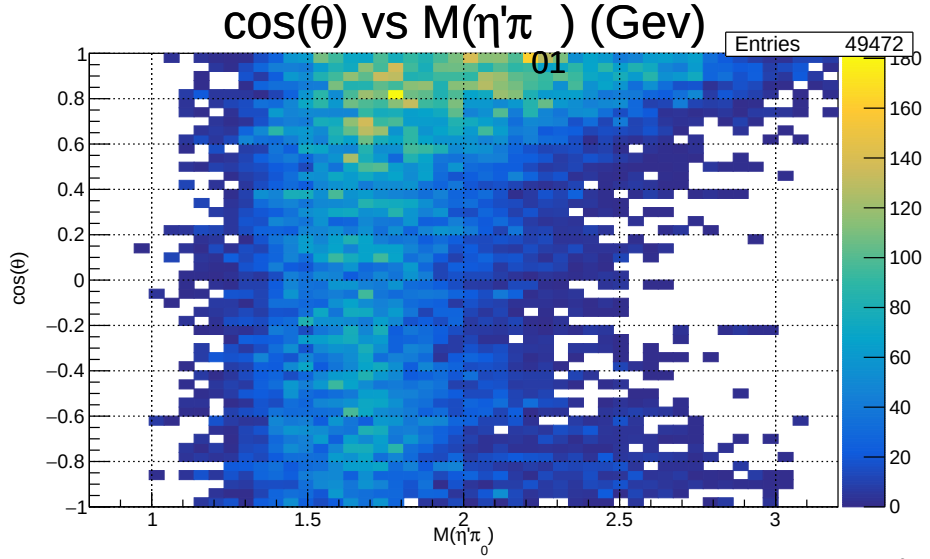

Figure 23: $\cos(\theta)$ of the η' particle in the Gottfried-Jackson Frame vs mass of $\eta'\pi^0$ GeV

acceptance would have to be studied and well understood in order to make a claim of an observation of the $\pi_1(1600)$. A poor understanding of the acceptance could lead to a false observation of the $\pi_1(1600)$. Studying the detector acceptance in this reaction requires a Monte Carlo simulation of the GlueX detector.

4 Conclusion

The goal of this work was to search for the hybrid $\pi_1(1600)$ decaying to $\eta'\pi^0$. This work was primarily exploratory, making the outcome of the analysis uncertain from the start. The first challenge was to reconstruct events with 8 photons and 3 charged tracks in the final state. We successfully reconstructed 4 π^0's, an η from 3 π^0's, and an η' from the η, π^+, and π^-. It also showed that η''s can be reconstructed enough to begin looking for hybrid mesons in this channel. Typically, the amount of background increases when more particles are added to the final state. Showing a nearly 6:1 ratio of signal to background in the η' mass means that this is a viable channel to search for hybrid mesons.

There are several things that were not accomplished in this analysis due to time constraints. Firstly, GlueX has approximately 10 times more data that can be analyzed. The same analysis could be run on this additional GlueX data and would directly lead to more total events in the final $\eta'\pi^0$, helpfully leading to more well defined peaks. This would allow for a clearer picture of what is going on and hopefully more defined spherical harmonics in $\cos(\theta)$ vs $M(\eta'\pi^0)$.

Secondly, longitudinal phase space plots, also known as Van Hove plots, can be contrasted of the final particles to make more cuts of the background data, further increasing the ratio of events to background. Thirdly, the process of side–band subtraction might be able to be preformed on the η and η' to extract only the signal from the data, further improving the signal to background ratio of η' events. Finally, one could begin studying data generated with Monte Carlo simulations of the GlueX detector to study the detector acceptance.

References

[1] S. Adhikari et al. "The GlueX beamline and detector". In: *Nuclear Instruments and Methods in Physics Research Section A: Accelerators, Spectrometers, Detectors and Associated Equipment* 987 (Jan. 2021), p. 164807. ISSN: 0168-9002. DOI: 10.1016/j.nima.2020.164807. URL: http://dx.doi.org/10.1016/j.nima.2020.164807.

[2] C. Adolph et al. "Odd and even partial waves of $\eta\pi^-$ and $\eta'\pi^-$ in $\pi^- p \to \eta^{(\prime)}\pi^- p$ at 191 GeV/c". In: *Phys. Lett. B* 740 (2015). [Erratum: Phys.Lett.B 811, 135913 (2020)], pp. 303–311. DOI: 10.1016/j.physletb.2014.11.058. arXiv: 1408.4286 [hep-ex].

[3] Rebecca Barsotti and Matthew R. Shepherd. "Using machine learning to separate hadronic and electromagnetic interactions in the GlueX forward calorimeter". In: *JINST* 15.05 (2020), P05021. DOI: 10.1088/1748-0221/15/05/P05021. arXiv: 2002.09530 [physics.data-an].

[4] R. Brun and F. Rademakers. "ROOT: An object oriented data analysis framework". Version 6.22/02. In: *Nucl. Instrum. Meth. A* 389 (1997). Ed. by M. Werlen and D. Perret-Gallix, pp. 81–86. DOI: 10.1016/S0168-9002(97)00048-X. URL: https://root.cern.

[5] Jozef J. Dudek et al. "Toward the excited isoscalar meson spectrum from lattice QCD". In: *Phys. Rev. D* 88.9 (2013), p. 094505. DOI: 10.1103/PhysRevD.88.094505. arXiv: 1309.2608 [hep-lat].

[6] Bernhard Ketzer. *Hybrid Mesons*. 2012. arXiv: 1208.5125 [hep-ex].

[7] C.A. Meyer and E.S. Swanson. "Hybrid mesons". In: *Progress in Particle and Nuclear Physics* 82 (May 2015), pp. 21–58. ISSN: 0146-6410. DOI: 10.1016/j.ppnp.2015.03.001. URL: http://dx.doi.org/10.1016/j.ppnp.2015.03.001.

[8] Curtis A Meyer. "Coordinate Systems in GlueX". In: (2020).

[9] P.A. Zyla et al. "Review of Particle Physics". In: *PTEP* 2020.8 (2020), p. 083C01. DOI: 10.1093/ptep/ptaa104.